Structure of Lactate Dehydrogenase from Plasmodium vivax : Complexes with NADH and APADH †

ARTICLE *in* BIOCHEMISTRY · JANUARY 2006

Impact Factor: 3.02 · DOI: 10.1021/bi051416y · Source: PubMed

6 AUTHORS, INCLUDING:

Rebecca Conners
University of Bristol
10 PUBLICATIONS **224** CITATIONS
SEE PROFILE

Dilek Turgut-Balik
Yildiz Technical University
38 PUBLICATIONS **277** CITATIONS
SEE PROFILE

Structure of Lactate Dehydrogenase from *Plasmodium vivax*: Complexes with NADH and APADH†

Apirat Chaikuad,‡ Victoria Fairweather,‡ Rebecca Conners,‡ Tim Joseph-Horne,‡ Dilek Turgut-Balik,§ and R. Leo Brady*,‡

Department of Biochemistry, University of Bristol, United Kingdom, and Department of Biology, University of Firat, Elazig, Turkey

Received July 20, 2005; Revised Manuscript Received September 21, 2005

ABSTRACT: Malaria caused by *Plasmodium vivax* is a major cause of global morbidity and, in rare cases, mortality. Lactate dehydrogenase is an essential *Plasmodium* protein and, therefore, a potential antimalarial drug target. Ideally, drugs directed against this target would be effective against both major species of *Plasmodium, P. falciparum* and *P. vivax*. In this study, the crystal structure of the lactate dehydrogenase protein from *P. vivax* has been solved and is compared to the equivalent structure from the *P. falciparum* enzyme. The active sites and cofactor binding pockets of both enzymes are found to be highly similar and differentiate these enzymes from their human counterparts. These structures suggest effective inhibition of both enzymes should be readily achievable with a common inhibitor. The crystal structures of both enzymes have also been solved in complex with the synthetic cofactor APADH. The unusual cofactor binding site in these *Plasmodium* enzymes is found to readily accommodate both NADH and APADH, explaining why the *Plasmodium* enzymes retain enzymatic activity in the presence of this synthetic cofactor.

Malaria caused by *Plasmodium vivax* is a major cause of morbidity in Africa, the Middle East, Asia, and Central and South America and is thought to account for 70−80 million cases annually. In the vast majority of infections, the disease caused by this parasite is not as severe as *Plasmodium falciparum* malaria and is rarely fatal, but has an immense negative impact on general health and quality of life, as well as creating a major economic burden for the people and countries affected (*1*). Characteristic symptoms of the disease include episodes of high fever accompanied by chills and rigor which are repeated every 48 h and which can last for weeks without treatment (*2*). *P. vivax* hypnozoites can also lie dormant within the liver and cause recurrences of disease years after the initial infection (*3*). Although unusual, severe complications can arise from *P. vivax* infections; a recent study in India reported the presence of cerebral malaria, renal failure, circulatory collapse, severe anaemia, haemoglobinurea, abnormal bleeding, acute respiratory distress syndrome, and jaundice in 11 patients who were shown to be infected with *P. vivax* only and not *P. falciparum* (*4*). In addition, *P. vivax* infections during pregnancy have been reported to be associated with low birthweight and subsequent increased neonatal mortality (*5*). With increasing research being targeted at developing cures for *P. falciparum* malaria, there is a potential for infections with the more robust *P. vivax* parasite to become more prevalent (*1*). The ideal situation would be for emerging antimalarial drugs to target both *P. falciparum* and *P. vivax* forms of malaria (*3*).

Lactate dehydrogenase is an essential enzyme for parasite survival as plasmodium lack a functional Krebs cycle during their erythrocytic stages and, hence, must generate all their energy from glycolysis coupled with fermentation (*6*). Lactate dehydrogenase catalyses the reduction of the keto group in pyruvate to a hydroxyl (yielding lactate) with the concomitant oxidation of NADH[1] to NAD^+. This regenerated NAD^+ is essential for the continuation of glycolysis. We have previously shown that a series of azole inhibitors of *P. falciparum* lactate dehydrogenase (*Pf*LDH) bind within the active site of the protein and inhibit enzyme activity in vitro and parasite growth in red blood cells and are also parasiticidal in vivo in a *Plasmodium berghei* rodent model (*7*). This series of compounds is selective for *Pf*LDH over the human LDH isoforms, and crystallographic studies have shown that the binding sites are conserved between the *P. falciparum* and *P. berghei* forms of LDH (*8*). This has provided the most compounding evidence so far that glycolysis and, specifically, LDH are viable targets for novel antimalarials.

† This work was supported by a DPST award from the Thai Government to A.C., and funding from the U.K. Biotechnology and Biological Sciences Research Council (R.C., T.J.-H., and R.L.B.) and from the Scientific and Technical Research Council of Turkey (TUBITAK), Project No. 104T215 (D.T.-B.).

* To whom correspondence should be addressed. E-mail: l.brady@bristol.ac.uk. Telephone: +44(117) 928-7436. Fax: +44(117) 928-8274.

‡ University of Bristol.

§ University of Firat.

[1] Abbreviations: LDH, lactate dehydrogenase; *Pv*LDH, *Plasmodium vivax* lactate dehydrogenase; *Pf*LDH, *Plasmodium falciparum* lactate dehydrogenase; *Pb*LDH, *Plasmodium berghei* lactate dehydrogenase; *Tg*LDH, *Toxoplasma gondii* lactate dehydrogenase; hLDH-A, human A-form lactate dehydrogenase; hLDH-B, human B-form lactate dehydrogenase; *Bs*LDH, *Bacillus stearothermophilus* lactate dehydrogenase; NADH, nicotinamide adenine dinucleotide, reduced; NAD^+, nicotinamide adenine dinucleotide, oxidized; $APAD^+$, 3-acetylpyridine adenine dinucleotide, oxidized; APADH, 3-acetylpyridine adenine dinucleotide, reduced; PDB, protein data bank; rms, root-mean-square.

10.1021/bi051416y CCC: $30.25
Published on Web 11/16/2005

As LDH is not unique to protozoa, it is crucial to develop drugs that have specificity for the malarial proteins over their human homologues. Protozoal LDHs display both structural and kinetic differences to their mammalian equivalents, and these might be exploited to develop drug selectivity. Structurally, plasmodial LDHs have a five residue insertion in their active site loop which closes down over the active site during catalysis and which is accompanied by a marked displacement (~1 Å) of the nicotinamide ring of the NADH cofactor (*9*, *10*), a feature also shared by the LDH1 from the related apicomplexan parasite *Toxoplasma gondii* (*11*). All plasmodial LDHs also differ in their kinetics from their mammalian counterparts. The latter have a pronounced propensity to be inhibited by excess levels of the substrate pyruvate, believed to result from slow release of the reduced cofactor NAD^+ and its subsequent formation of a covalent adduct with pyruvate within the active site (*12*). The significant reduction in substrate inhibition associated with plasmodial LDHs has been suggested to result from the substitution of a single amino acid (Ser163Leu) (*13*), although a more recent comparison of the enzymatic activities of four forms of plasmodial LDH notes that a range of molecular features are likely to be involved (*14*). A further kinetic feature of the plasmodial LDHs is their ability to efficiently use the synthetic coenzyme 3-acetylpyridine adenine dinucleotide (APAD) as a cofactor. As turnover of APAD is more restricted for mammalian LDHs, APAD has been used as the basis for a clinical test for malaria (*15*). At high lactate concentrations, plasmodial LDHs are 500 times more active with APAD than human LDH (*16*).

A recent study (*14*) has reported a detailed enzymatic characterization of the LDH enzymes from all four species of the Plasmodium parasite known to infect humans, and included predicted model structures of three of these enzymes, based on the crystal structure (*9*) of the fourth, *P. falciparum* LDH (*Pf*LDH). In this study, we report a crystal structure of the lactate dehydrogenase from *P. vivax* (*Pv*LDH). The structure of this enzyme has been determined in two forms, in complex with NADH and in complex with the alternative cofactor, APADH. For comparative purposes, we have also determined the structure of *P. falciparum* LDH complexed with APADH. Together with kinetic characterization studies, these structures enable a direct assessment of the common structural features shared by this potential antimalarial drug target from the two most important plasmodial strains known to infect humans. In addition, detailed structural knowledge of the specific binding mode of APADH to malarial LDHs adds to the existing, largely kinetic, studies exploring the preferential utilization of this cofactor by the malarial enzymes.

EXPERIMENTAL PROCEDURES

Protein Production and Purification. Recombinant *Pv*LDH (Belem strain) and *Pf*LDH were expressed as described previously (*17*, *18*) and purified on a HiTrap Ni^{2+} column (GE Bioscience) using a 0.02−1 M imidazole gradient. The resulting pure protein (>95% purity by SDS−PAGE analysis) was buffer exchanged into 100 mM Na Hepes, 100 mM imidazole, 5% glycerol, and 5 mM β-mercaptoethanol, pH 7.5, and concentrated to 20 mg/mL in a 30 kDa Vivaspin (Vivascience). Both constructs consisted of the LDH protein plus a small poly-histidine tag of six residues on the C-terminus which was not cleaved prior to crystallization.

*Crystallization. Pv*LDH was incubated with 2 mM NADH and 1 mM oxamate (Sigma) and subjected to a sparse matrix crystallization screen (Structure Screen 1 and 2, Molecular Dimensions Ltd.) using the hanging drop method of vapor diffusion. The best crystals were improved by further screening and the optimal conditions found to be 20−30% PEG 5000 monoethyl ether, 0.2 M ammonium sulfate, and 0.1 M Mes, pH 6.1, with a protein concentration of 13.45 mg/mL. The same conditions were used to grow the *Pv*LDH−APADH crystal, with a 3 h incubation of 12 mM APADH replacing NADH. The *Pf*LDH−APADH cocrystal grew in 50% 2-methyl-2,4-pentanediol at a protein concentration of 5 mg/mL following incubation of protein with 12 mM APADH overnight at room temperature.

Data Collection and Structure Refinement. Crystals were cryoprotected with mother liquor and 15% glycerol (*Pv*LDH), or mother liquor alone (*Pf*LDH), and cooled to 100 K in a liquid nitrogen cryostream (Oxford Cryosystems) for data collection. Data were collected at Daresbury SRS PX14.1 (*Pv*LDH−NADH and *Pv*LDH−APADH) and PX14.2 (*Pf*LDH−APADH). Data were processed and scaled with HKL2000 (*19*).

*Pv*LDH crystals were found to belong to a primitive orthorhombic Bravais lattice with unit cell dimensions $a = 81.6$, $b = 128.6$, $c = 130.6$, $\alpha = \beta = \gamma = 90°$ (*Pv*LDH−NADH complex) and $a = 81.5$, $b = 128.5$, $c = 130.8$, $\alpha = \beta = \gamma = 90°$ (*Pv*LDH−APADH complex). Subsequent inspection of the systematic absences revealed the spacegroup to be $P2_12_12_1$. The spacegroup of the *Pf*LDH−APADH crystals was $I222$ ($a = 80.2$, $b = 86.2$, $c = 90.8$, $\alpha = \beta = \gamma = 90°$) as previously described for *Pf*LDH−NADH (*9*). Structures were solved by molecular replacement using the program AMORE (*20*) and the binary structure of *Pf*LDH (1T2C.pdb) with ligands and waters removed as a search model. The structures were refined using REFMAC5 from the CCP4 suite of crystallographic software (*21*) and rebuilt with QUANTA (Accelrys Inc., San Diego, CA) (*Pf*LDH−APADH) and COOT (*Pv*LDH−NADH and *Pv*LDH−APADH) (*22*). Four hundred and eighty water molecules and four molecules of NADH have been included in the final model for the *Pv*LDH−NADH complex, 479 waters and four APADH molecules in the *Pv*LDH−APADH structure, and 219 waters and one APADH molecule in the *Pf*LDH−APADH structure. Completed structures were checked for geometric correctness with PROCHECK (*23*) and WATCHECK (*24*). Data collection and refinement statistics are summarized in Table 1. The coordinates and structure factors have been deposited with the PDB (accession codes 2A92, 2AA3, and 2A94).

Steady-State Enzyme Kinetics. K_M values for pyruvate, NADH, and APADH were measured by monitoring the change in absorbance of cofactor at 340 nm at pH 7.5 as described previously (*8*). Assays were performed in a 100 μL volume using an enzyme concentration of 3 nM. The K_M for pyruvate was determined with a range of pyruvate concentrations from 0.01 to 100 mM and an NADH concentration of 200 μM. The K_M for NADH/APADH was measured using cofactor concentrations from 0.01 to 0.8 mM and a pyruvate concentation of 500 μM. Corrections were made for background turnover, and data were fitted to the

Table 1: Data Collection and Refinement Statistics for *Pv*LDH−NADH, *Pv*LDH−APADH, and *Pf*LDH-APADH Complexes[a]

complex	*Pv*LDH−NADH	*Pv*LDH−APADH	*Pf*LDH−APADH
PDB accession code	2A92	2AA3	2A94
Daresbury SRS Beamline	14.1	14.1	14.2
spacegroup	$P2_12_12_1$	$P2_12_12_1$	$I222$
resolution range (Å)	30.0−2.00 (2.10−2.00)	50.0−2.05 (2.15−2.05)	30.0−1.50 (1.62−1.50)
no. unique reflections	85851	85446	50501
completeness (%)	98.2 (97.5)	98.4 (96.9)	99.5 (99.5)
redundancy	3.9 (3.8)	8.2 (7.8)	4.5 (4.1)
$I/\sigma I$	11.8 (2.4)	21.3 (4.6)	37.4 (7.3)
R_{sym}	0.108 (0.434)	0.099 (0.379)	0.031 (0.133)
R_{cryst}	0.194	0.190	0.160
R_{free}	0.236	0.226	0.176
rms deviation bond length (Å)	0.015	0.023	0.012
rms deviation bond angle (deg)	1.525	1.829	1.533

[a] Numbers in parentheses show the statistics for the highest resolution shell; PDB indicates protein data bank, and rms indicates root-mean-square.

Michaelis−Menten equation (corrected for substrate inhibition: $V/V_{max} = S/[S + K_M + (S^2/K_i)]$) using the nonlinear regression facility in Grafit 3.0 (*25*).

RESULTS

P. vivax Lactate Dehydrogenase Complexed with NADH. The *Pv*LDH structure consists of a tetramer in the asymmetric unit with each monomer displaying the typical two-domain LDH fold (Figure 1). The first, and largest, domain forms a Rossmann fold and binds the NADH cofactor, while the catalytic residues are found within the second domain. The active site of the enzyme is located between these two domains. There are four molecules of NADH present in the tetramer, one in each monomer, and superposition of the four protein chains shows that these cofactor molecules are found in an identical position in each subunit.

These crystals containing a binary (NADH−*Pv*LDH) complex were grown in the presence of both NADH and oxamate and were therefore expected to yield ternary (oxamate−NADH−*Pv*LDH) complexes. There are two major structural differences between binary and ternary *Pf*LDH complexes. First, in ternary complexes, the active site loop (residues 100−110) has distinctive electron density and closes down over the substrate, whereas in binary complexes, this loop is completely disordered. Second, it has been noted from previous *Pf*LDH complexes that a second loop (containing Ser 245/Pro 246) also changes conformation between binary and ternary complexes. When oxamate or a small azole inhibitor is bound within the active site, this loop adopts a "closed" conformation with Ser 245 pointing directly into the active site and forming a hydrogen bond with the inhibitor (*7*). With an "empty" active site (occupied by water molecules), this loop is "open", and the serine hydroxyl group points away from the binding site (Figure 1, inset). In the *Pv*LDH−NADH and *Pv*LDH−APADH structures, three molecules have completely disordered active site loops, and the fourth takes on a nonternary conformation due to crystal contacts. Two molecules have their Ser 245 hydroxyl groups pointing away from the active site and two have them pointing toward the active site. The presence of the disordered active site loop, and the "open" conformation Ser 245, enabled us to be certain that these crystals were truly binary, and the electron density observed within the active site was modeled as water molecules rather than oxamate. It is conceivable that crystal contacts prevent the formation of ternary complexes in this crystal form, as closure of the active site would disrupt the existing crystal contacts. This particular crystal form appears to be selective for binary complexes.

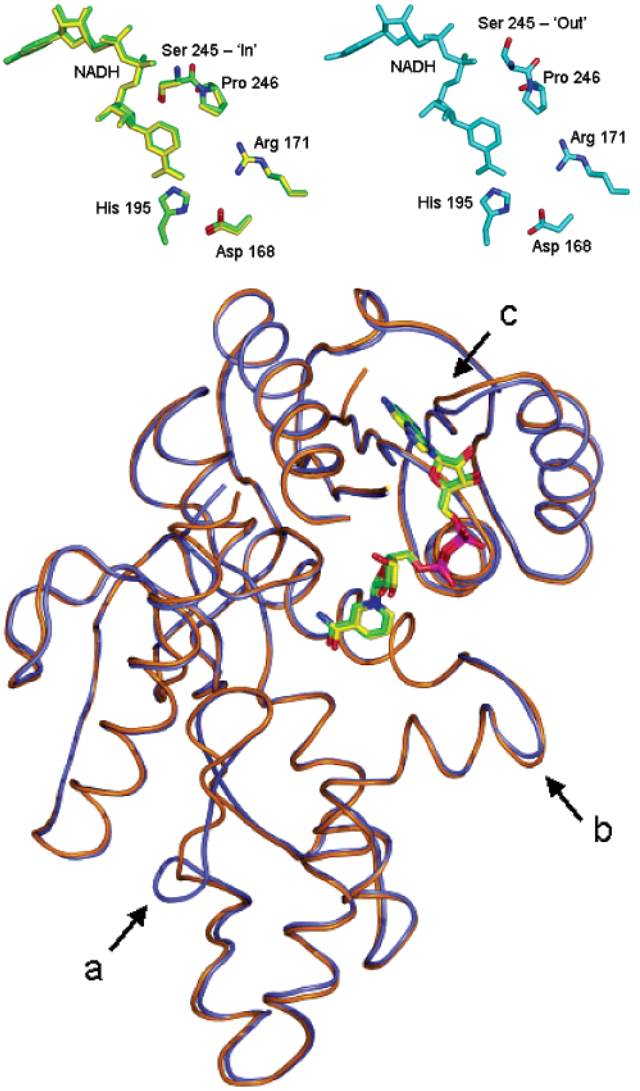

FIGURE 1: Overlay of *Pv*LDH−NADH and *Pf*LDH−NADH complexes. *Pv*LDH is shown in blue and *Pf*LDH in orange with *Pv*LDH NADH in yellow and *Pf*LDH NADH in green. The overall structure is highly conserved between the two plasmodial proteins. There are small differences in loop 198−223 (a), 237−246 (b), and 53−62 (c). Inset shows the two different conformations of Ser 245 observed within this crystal form. Chain A is shown in green, chain C in yellow, and chain D in cyan. Chain B is not shown, as there was no observable electron density for the Ser 245 side chain. Chains A and C depict the "in" mode and chain D depicts the "out" mode, with reference to the position of the serine side chain. See text for a further description of these terms and ref *7* for a detailed explanation. All figures were created with Pymol (*34*).

P. vivax Lactate Dehydrogenase Complexed with APADH. Crystals of this complex belong to the same crystal form as the *Pv*LDH−NADH crystals. Residues 100−110 (corre-

Table 2: Steady-State Kinetic Data for Selected Recombinant LDH Enzymes

	cofactor	*Pv*LDH	*Pf*LDH	hLDH-A	hLDH-B	*Tg*LDH1
K_M, pyruvate (μM)	NADH	52 ± 2	51 ± 2	170[a]	55[a]	359[b]
	APADH	121 ± 18	121 ± 15	-	-	814[b]
K_i, pyruvate (mM)	NADH	25 ± 2	82 ± 5	0.77[c]	3.9[d]	31[b]
	APADH	2.2 ± 0.3	2.4 ± 0.3	-	-	25[c]
k_{cat}, pyruvate (s^{-1})	NADH	32 ± 1 (127)[e]	32 ± 1 (148)[e]	300[a]	220[a]	64[e]
	APADH	6.0 ± 0.8	11.3 ±.2.0			30[e]
k_{cat}/K_M, pyruvate ($s^{-1} M^{-1}$)	NADH	6.2×10^5 (7.3×10^5)[e]	6.3×10^5 (5.0×10^6)[e]	(1.8×10^6)[a]	(4.0×10^6)[a]	(1.8×10^6)[e]
	APADH	5.0×10^4	9.3×10^4			(3.7×10^4)[e]
K_M, NADH (μM)		22 ± 1 (7 ± 1.1)[a]	26 ± 1 (7 ± 0.8)[a]	5[a]	8[a]	4.2[f]
K_M, APADH (μM)		24 ± 1	22 ± 6			-

[a] From ref *28*. [b] From ref *11*. [c] From ref *32*. [d] From ref *13*. [e] From ref *14*. [f] From ref *33*.

sponding to the active site loop) and those at the N- and C-termini are disordered and were included in the model at zero occupancy. There is partial ordering of the active site loop in one molecule due to crystal contacts. One molecule of APADH is bound with full occupancy to each chain.

P. falciparum Lactate Dehydrogenase Complexed with APADH. The *Pf*LDH−APADH complex has one molecule in the asymmetric unit, and therefore, each molecule in the tetramer is identical. Residues 100−110 of the active site loop were disordered but included in the model at zero occupancy, and one molecule of APADH was bound with full occupancy.

Kinetic Analyses. Preliminary steady-state kinetic parameters obtained for *Pv*LDH with pyruvate, NADH, and APADH are summarized in Table 2, which also includes comparable published values for *Pf*LDH, *Tg*LDH, and human hLDH-A and hLDH-B, where available. The results obtained in this study were from the recombinant form of *Pv*LDH which includes the $(His)_6$-affinity tag.

DISCUSSION

Plasmodium Lactate Dehydrogenases Are Closely Related in Structure. The four human malaria parasites differ greatly in their morphology and resulting disease symptoms, although ideally could be treated via a common molecular target. *Pv*LDH shares 89% sequence identity with *Pf*LDH, with the majority of residue changes being restricted to the surface of the protein. None of these changes lead to significant alterations in the overall conformations of the two proteins: all *Pf*LDH and *Pv*LDH Cα residues (excepting those in the active site loop) align with a root-mean-square (rms) deviation of 0.88 Å. By comparison, *P. berghei* LDH (*Pb*LDH), from a *Plasmodium* species that causes rodent malaria and is frequently used as a model for human *P. falciparum* infection, is even more closely related to *Pf*LDH (97% sequence identity, rms deviation of 0.37 Å over all Cα atoms (*8*)) Figure 1 shows the models for the *Pv*LDH−NADH and *Pf*LDH−NADH (1T2C.pdb) binary complexes superimposed.

Minor conformational differences are seen in loops 198−223 (labeled (a) in Figure 1), 237−246 (labeled (b)), and 53−62 (labeled (c)), the latter two regions contributing to the cofactor binding site. Loop 198−223 contains a number of amino acid differences between the two plasmodial proteins but is situated distant from the active site. Loop 237−246 contains the mobile Ser 245 which has been observed to adopt different conformations in binary and ternary complexes (see inset to Figure 1) and known to be a region of high mobility (*7*). There is a nonconservative His → Leu substitution at position 243 of this loop. In *Pf*LDH, the histidine forms a weak (3.1 Å) hydrogen bond with the hydroxyl of tyrosine 247; loss of this interaction with the leucine side chain seems unlikely to be significant. Nonetheless, the change from a potentially charged group to a nonionizable group close to the active site might influence the pH optima of the enzyme as demonstrated for the two major human isoforms of LDH (*10*). Conformational changes in the 53−62 region are also potentially important, as this loop packs against the adenyl ring of the NADH cofactor. This region is the site of chloroquine binding to *Pf*LDH (*26*). Position 54 is valine in *Pv*LDH and isoleucine in *Pf*LDH (Figure 2a). In both cases, these hydrophobic side chains stack against the adenyl ring of NADH, presumably explaining the small displacement (0.3 Å) of this ring observed between these complexes. However, movement of the adenyl ring is frequently observed in LDH crystal structures. By comparison, alignment of the active site side chains (Arg 171, His 195, and Asp 168) shows a near-identical binding of the NADH nicotinamide and phosphate moieties for both species (Figure 2b).

Although not observed in these binary *Pv*LDH complexes, the *P. falciparum* and *P. vivax* forms of the enzyme also differ by a nonconservative Leu → Asp 110 substitution within the active site loop. By analogy with the structure of the *Pf*LDH ternary complex (*9*), the aspartate at position 110 of *Pv*LDH is expected to lie along the surface of the protein and not participate directly in the active site. As no significant change in catalytic activity was observed between *Pv*LDH and *Pf*LDH, we conclude that this substitution is unlikely to alter the enzyme structure.

In sum, the crystal structures of *Pv*LDH, *Pf*LDH, and *Pb*LDH show these enzymes all share highly similar structures, with no significant alterations observed within the active site or cofactor binding pocket. This conservation of structure correlates with their closely comparable activity profiles. Inhibitors targeting the active site region of these enzymes are therefore likely to be effective across the *Plasmodium* genus.

Cofactor Binding Differs between Plasmodium and Human Lactate Dehydrogenases. Ideally, antimicrobial molecular targets should be unique to the pathogen. However, exclusivity might also be achieved through a target which, although

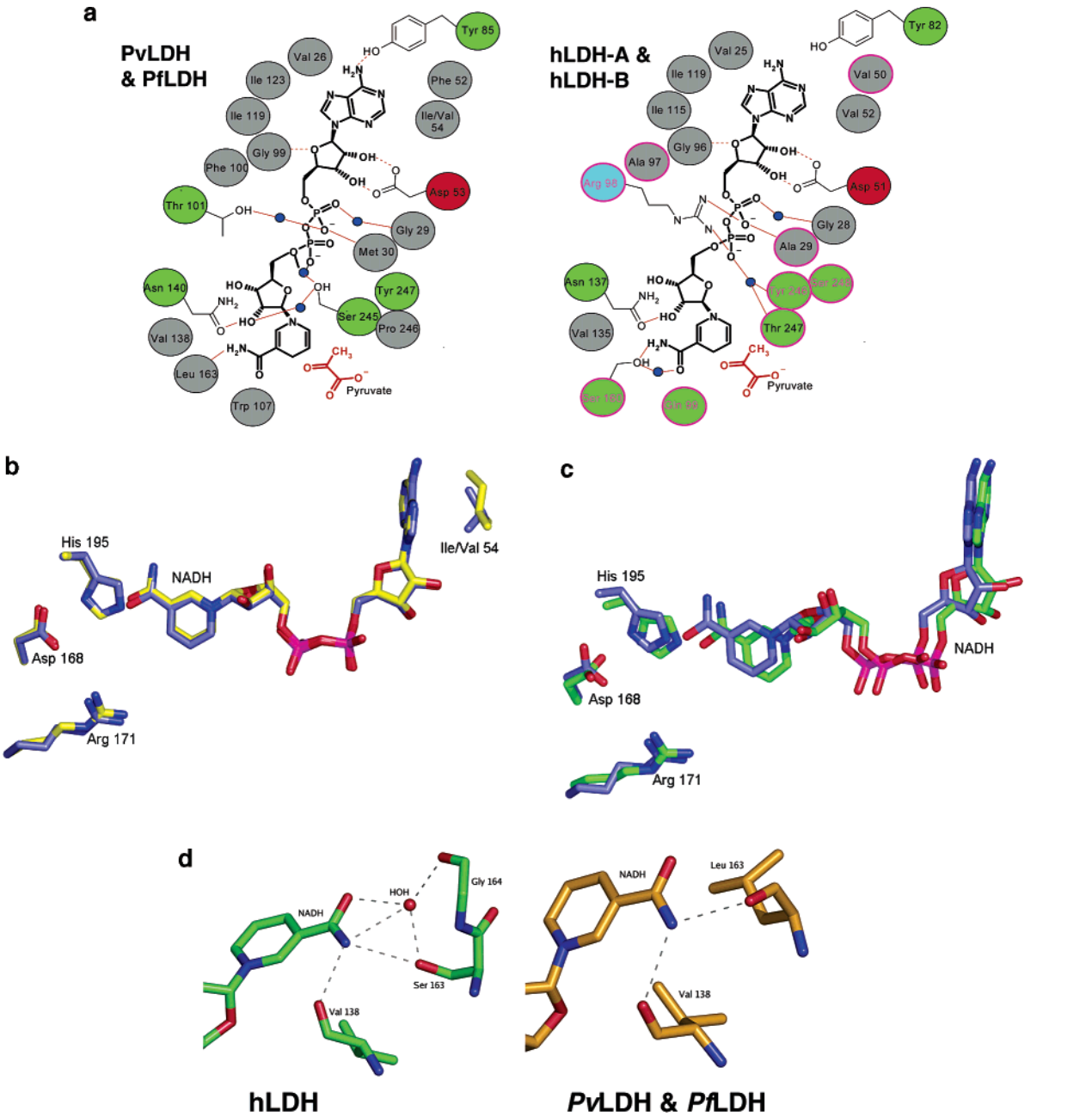

FIGURE 2: Cofactor placement in *Plasmodium* and human LDH enzymes. (a) Schematic diagram showing the cofactor binding pocket in (left) *Plasmodium* and (right) human LDHs. Most amino acids that form either van der Waals contacts or hydrogen bonds (dashed red lines, to main-chain amide groups unless side chain shown) with the NADH cofactor are represented by spheres, colored gray for nonpolar, green for uncharged polar, blue for positively charged, and red for negatively charged amino acids. Bound water molecules are shown as small spheres in dark blue. Significant changes in types of amino acid are highlighted in magenta in the diagram for human LDH; these changes cluster toward the nicotinamide end of the cofactor. The conserved catalytic residues have been omitted for clarity. (b) Overlay of NADH from *Pv*LDH−NADH (blue) and *Pf*LDH−NADH (yellow) complexes with catalytic residues shown. Residue 54 is an isoleucine in *Pv*LDH and a valine in *Pf*LDH. (c) Overlay of NADH from *Pv*LDH−NADH (blue) and human LDHA−NADH (green) complexes with catalytic residues shown. The LDHA cofactor is displaced by approximately 1.0 Å compared to that of *Pv*LDH. (d) Detail of binding interactions between the nicotinamide group and 163 and surrounding residues. Left panel (green) shows the arrangement for human (and all nonapicomplexan) LDHs; right panel (gold) shows the same region from the two *Plasmodium* LDH structures. Hydrogen bonds are shown as dashed lines, and the conserved bound water molecule is shown as a red sphere.

common to both host and pathogen, has a sufficiently different molecular structure. *Plasmodium* LDHs are more distantly related to their mammalian counterparts (*Pv*LDH and *Pf*LDH share 26 and 29% sequence identity with human A LDH (hLDH-A), respectively) although the catalytic residues (Arg 109, Arg 171, His 195, and Asp 168) are strictly conserved. Alignment of all Cα residues shows an rms deviation of 2.2 Å between *Pv*LDH and hLDH-A and 2.3 Å between *Pf*LDH and hLDH-A. In addition to the characteristic five-residue insertion in the active site loop, the *Plasmodium* LDH enzymes also feature a number of substitutions in the cofactor-binding groove that distinguish *Plasmodium* and human forms of LDH. Whereas (apart from the conservative substitution of valine for isoleucine at position 54) the composition and conformation of all residues lining the cofactor binding site is identical between *Pv*LDh and *Pf*LDH, there are at least nine positions where there are changes with the human LDH structures. These changes are

evident in the schematic shown in Figure 2a. In particular, the 245−247 loop and positions 163 and 107 (underside of active site loop) differ substantially between the *Plasmodium* and mammalian enzymes. As can be observed in the figure, these residues cluster around the nicotinamide binding site of the cofactor pocket. We note this is the region in which inhibitors selective for *Pf*LDH and *Pb*LDH over human LDHs have been reported to bind (*7*).

The cumulative effect of these changes is perhaps best illustrated by comparing the bound conformation of an identical ligand, the cofactor NADH. The kinetic data in Table 2 show that *Pf*LDH and *Pv*LDH bind NADH with similar affinity, albeit approximately 5-fold less tightly than does hLDH-A. When the active site residues of *Pv*LDH are overlaid with those of hLDH-A, it becomes evident that the cofactor is displaced within the binding pocket, relative to its location in complexes with human (and all other nonapicomplast) LDH enzymes (Figure 2c). This displacement is most pronounced in the nicotinamide moiety, which is shifted by about 1 Å relative to its position in the hLDH-A structure. This phenomenon is also observed with *Pf*LDH (Figure 2b), *Pb*LDH, and *Tg*LDH (*8*, *9*, *11*) and highlights that these key differences between apicomplast and mammalian enzyme cofactor binding sites alter the association of these enzymes with their ligands. This feature could be used as the basis for selective inhibition of *Plasmodium* LDHs. We have recently recorded details of a group of gossypol-like compounds which bind within the cofactor-binding site and weakly inhibit LDH activity (*27*). Although these compounds are not specific for *Plasmodium* LDH, they prove that inhibition of the protein can be obtained by targeting this site, and the presence of a cluster of amino acid differences within this region increases the potential for creating specificity. A series of gossypol derivatives have been demonstrated to bind competitively with NADH to all four human plasmodial LDH enzymes (*14*), consistent with the structures of the naphthoic acid based complexes reported in ref *27*.

Reduced Substrate Inhibition. Consistent with other published studies (*14*, *28*), Table 2 shows that *Pv*LDH is similar to *Pf*LDH in exhibiting reduced pyruvate substrate inhibition. Some variation from other published values might be expected, as the recombinant proteins used in this study all retained $(His)_6$ tags. Although the K_i for pyruvate with NADH in this study is lower for *Pv*LDH (25 mM) compared with that for *Pf*LDH (82 mM) and comparable to the value reported for *Tg*LDH1 (31 mM), these values are at least an order of magnitude greater than the equivalent values from the two major human isoforms (hLDH-A, 0.77 mM; hLDH-B, 3.9 mM). Interestingly, we find that this effect is much reduced when APADH is used as cofactor, unlike the data reported for *Tg*LDH1 (*11*).

Many studies have addressed the molecular basis of pyruvate inhibition of LDHs, believed to result from the enol form of pyruvate forming a covalent adduct with NAD^+ within the active site (*13*). Slow release of cofactor is thought to be an important factor. A crucial experiment (*13*, *29*) was the demonstration that substrate inhibition could be relieved in the *Bacillus stearothermophilus* enzyme (*Bs*LDH) through the simple mutation of the serine at position 163 to a leucine, as found in *Pf*LDH which was known to have an increased K_i for pyruvate (*30*). Studies (*13*) indicated that the low level of substrate inhibition displayed by a similar mutant of hLDH-A could be attributed to the weaker binding of pyruvate to the enzyme−NAD^+ complex. Nonetheless, other studies (*14*, *28*) indicate that the phenomenon is likely to be more complex in the *Plasmodium* enzymes than suggested by the simple mutational studies. Kinetic data for all four plasmodial LDHs show that the binding of pyruvate is similar to human LDHs (*14*). Similarly, the K_M values for NAD^+ binding to *Pf*LDH and human LDHs are comparable (*28*).

In conventional LDHs, the serine side chain at position 163 is central to the formation of a complex network of six hydrogen bonds between the nicotinamide ring substituent, solvent, and the enzyme. The serine hydroxyl forms a hydrogen bond with the cofactor nicotinamide amine group, in addition to a bifurcated hydrogen bond to a conserved water molecule also bridging the amide oxygen from the nicotinamide substituent and amide oxygen of the adjacent Gly164 (see Figure 2d). In *Pf*LDH, it was noted (*9*) that inclusion of the bulky, hydrophobic leucine side chain at position 163 inverts the conformation of the main chain in this region (the ψ angle is about 120°, compared with ∼25° in the mammalian LDHs). This results in the main-chain carbonyl group of Leu 163 being similarly located to the Ser 163 hydroxyl group in human LDH; however, the same network of interactions is not present, and the conserved water binding site is disrupted. The altered association of the cofactor with the enzyme (discussed above) results in the bound nicotinamide ring being placed closer to the 163/164 main chain (hence occluding the water site) but, additionally, pushes the ring into the pyruvate binding site by about 0.5 Å. A similar phenomenon is also observed in *Pb*LDH (*8*), *Tg*LDH (*14*) (which has a methionine at 163), and now, in this study, also in *Pv*LDH (Figure 2). We note from this study that the *Plasmodium* enzymes all appear to have evolved to allow substrate turnover with the nicotinamide group in closer proximity to the substrate site. This structural perturbation may be influential in the reduction of substrate inhibition. It is possible that the small distortion in the local geometry caused by the altered placement of the nicotinamide ring in these enzymes creates a less favorable environment for adduct stabilization. Further studies are required to fully understand this complex phenomenon.

APADH Association with Plasmodium and Human LDH. The ability of *Plasmodium* LDHs to use APADH as a cofactor is the basis of a clinical test for malaria, exploiting the observation that the *Plasmodium* enzymes are over 500 times more active with APADH than human LDHs (*16*). An increased entropic component associated with APADH binding, altered rate of active site loop movement, and higher oxidation potential of $APAD^+$ has previously been proposed to explain the tolerance of *Plasmodium* and related dehydrogenases for the APADH cofactor (*11*, *14*, *31*). APADH is a synthetic NADH analogue which has a methyl group replacing the nicotinamide amide nitrogen (Figure 3a). In NADH−hLDH complexes, this amido group normally participates in the complex network of hydrogen bonds involving the Ser 163 side chain, bound water molecule, and main-chain carbonyls of both Gly 161 and Val 138 (Figure 2d) locating the nicotinamide ring within the cofactor pocket. In comparison, although the *Plasmodium* LDHs bind NADH with similar affinity (Table 2), binding must be achieved

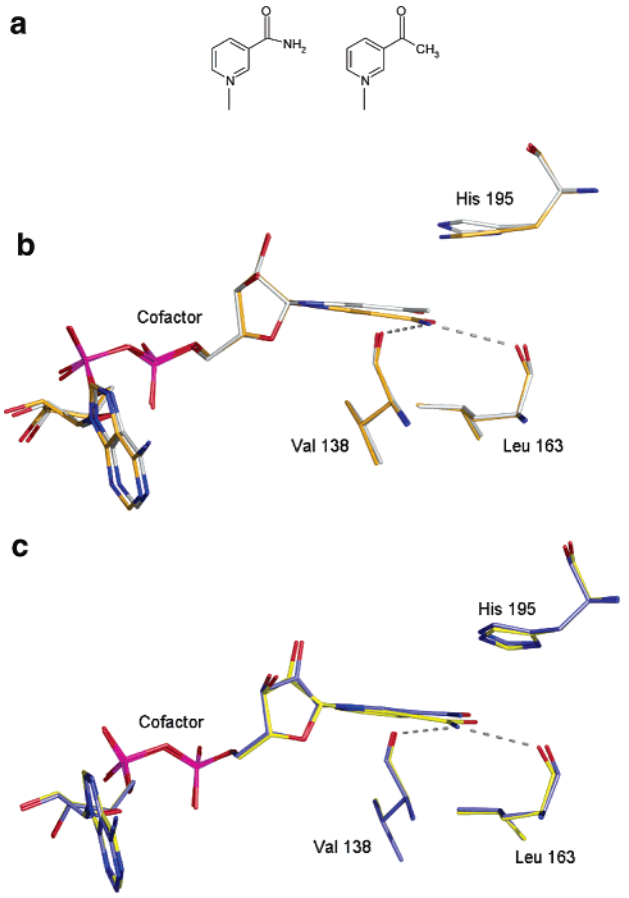

FIGURE 3: Placement of APADH and NADH in Plasmodial LDH enzymes. (a) Schematic showing the chemical composition of the nicotinamide ring of NADH and the equivalent acetyl-pyridine ring in APADH. The nicotinamide amine group is replaced by an acetyl group in APADH. (b) Overlay of *Pf*LDH−APADH (white) and *Pf*LDH−NADH (orange) structures. There is a displacement (0.45 Å) of both the acetyl-pyridine ring of APADH and of the imidazole ring of His 195 in the APADH structure when compared to the NADH structure. Leu 163 is a serine in the human enzyme and hydrogen bonds to the amine group of NADH. (c) Overlay of *Pv*LDH−APADH (blue) and *Pv*LDH−NADH (yellow) structures. There is a displacement of 0.3 Å of both the acetyl-pyridine ring of APADH and the imidazole ring of His 195 when compared to the NADH structure.

through a greater entropic component or increased van der Waals contacts, as the altered geometry arising from the inclusion of leucine at 163 creates a more hydrophobic pocket in which only two hydrogen bonds are formed (Figure 2d). In all APADH−LDH complexes, the nicotinamide amido group nitrogen is not present to form hydrogen bonds. Consequently, APADH forms a poor substrate for human LDHs (*13*), as the expected six hydrogen bonds within the pocket cannot form. In contrast, association of APADH with *Plasmodium* LDHs results in the loss of only two hydrogen bonds, cofactor binding is barely disrupted, and catalysis can still proceed efficiently.

The current study affords two comparative views of APADH and NADH binding, to both *Pv*LDH and *Pf*LDH, to support this structural explanation of APADH tolerance in the *Plasmodium* enzymes. In each case, we have compared binary complexes, but as catalysis proceeds via an ordered mechanism in which the cofactor binds before substrate, the placement of the cofactor is not expected to be altered between binary and ternary complexes. This has been confirmed by a comparison of the *Pf*LDH−NADH and *Pf*LDH−NADH−oxamate structures (*7*).

Alignment of the active site residue Cα atoms of *Pf*LDH−APADH and *Pf*LDH−NADH shows a near-identical overlay of each complex, with the only evident change being a small displacement of the nicotinamide rings of the cofactors (Figure 3b). To accommodate the inclusion of the methyl group and loss of the hydrogen bond to the Leu 163 carbonyl, the APADH nicotinamide rings tilt away from Val 138, and hence once again toward the pyruvate binding site, by about 0.5 Å. Concerted, very small changes in the active site amino acids are seen, the most significant being the imidazole ring of His 195 which moves 0.5 Å along with the shift of the nicotinamide group. This conserves the hydrogen bond between the NADH amide oxygen and the histidine NE2 nitrogen (bond distances are 3.1 Å for APADH and 3.0 Å for NADH complexes). Similarly, when the *Pv*LDH−APADH and *Pv*LDH−NADH complexes are compared (Figure 3c), once again the most significant change is in the amide group of NADH and the acetyl group of APADH. In APADH, the acetyl group moves toward the pyruvate site by about 0.3 Å, and again, the active site His 195 moves along with this group to maintain its hydrogen bond link.

Although these are very small changes, there are several reasons to believe them to be real. First, the changes are consistent between both the *Pf*LDH and *Pv*LDH complexes (Figure 3). Second, in the structure of *Tg*LDH complexed with $APAD^+$, a 7° torsional rotation of the pyridine ring causes the methyl group to move further away from the backbone carbonyl groups of Val 138 and Met 163 by similar amounts (*11*). Finally, the changes we observe are also consistent with those noted by Reddy et al. (*31*) in their study of NADH and APADH complexes of *Escherichia coli* dihydrodipicolinate reductase.

As previously described for *Tg*LDH (*11*), we also find the K_M for pyruvate in the presence of APADH is about double that in the presence of NADH (Table 2). This is consistent with a destabilized APADH ternary complex relative to the NADH ternary complex, correlating with the small structural perturbations observed in the *Pf*LDH−APADH and *Pv*LDH−APADH complexes in this study. Differences in the oxidation potential of $NAD^+/APAD^+$ have also been proposed (*11*) to explain the altered enzymatic activities with these cofactors. The accommodation of the APADH cofactor in a very similar position to NADH in the *Plasmodium* enzymes, inducing only a very small rearrangement of the critical active site residue His 195, is consistent with both of the above explanations.

SUMMARY

This study describes the crystal structure of lactate dehydrogenase from *P. vivax*, the causative agent of *vivax* malaria. The crystal structure of *P. vivax* LDH confirms a series of characteristic structural features that distinguish apicomplexa LDH enzymes from their mammalian counterparts, supporting their suitability for targeting in drug design studies.

Close structural similarity is found between the lactate dehydrogenases from *P. vivax* and *P. falciparum*, especially within the active site cleft. This indicates that inhibitors targeting this region of either of these proteins are also likely

to inhibit the other enzyme. Structures of both *P. falciparum* and *P. vivax* LDH complexed with the synthetic cofactor APADH have also been determined. Although very small movements of the nicotinamide group are associated with each cofactor, overall both NADH and APADH are bound by both enzymes in a very similar manner. This correlates with the general tolerance of the APADH cofactor that distinguishes the *Plasmodium* LDHs from their human homologues.

ACKNOWLEDGMENT

We thank the staff at the Daresbury SRS synchrotron for access to and assistance with X-ray facilities, Drs. Jon Read and Gus Cameron for their contributions to the *Pf*LDH−APADH studies, and Drs. Debbie Shoemark and Richard Sessions for help and advice with the kinetic studies.

REFERENCES

1. Mendis, K., Sina, B. J., Marchesini, P., and Carter, R. (2001) The neglected burden of *Plasmodium vivax* malaria, *Am. J. Trop. Med. Hyg. 64*, 97−106.
2. Karunaweera, N. D., Grau, G. E., Gamage, P., Carter, R., and Mendis, K. N. (1992) Dynamics of fever and serum levels of tumor necrosis factor are closely associated during clinical paroxysms in *Plasmodium vivax* malaria, *Proc. Natl. Acad. Sci. U.S.A. 89*, 3200−3203.
3. Ridley, R. G. (2002) Chemotherapeutic hope on the horizon for *Plasmodium vivax* malaria? *Proc. Natl. Acad. Sci. U.S.A. 99*, 13362−13364.
4. Kochar, D. K., Saxena, V., Singh, N., Kochar, S. K., Kumar, S. V., and Das, A. (2005) *Plasmodium vivax* malaria, *Emerging Infect. Dis. 11*, 132−134.
5. Nosten, F., McGready, R., Simpson, J. A., Thwai, K. L., Balkan, S., Cho, T., Hkirijaroen, L., Looareesuwan, S., and White, N. J. (1999) Effects of *Plasmodium vivax* malaria in pregnancy, *Lancet 354*, 546−549.
6. Lang-Unnasch, N., and Murphy, A. D. (1998) Metabolic changes of the malaria parasite during the transition from the human to the mosquito host, *Annu. Rev. Microbiol. 52*, 561−590.
7. Cameron, A., Read, J., Tranter, R., Winter, V. J., Sessions, R. B., Brady, R. L., Vivas, L., Easton, A., Kendrick, H., Croft, S. L., Barros, D., Lavandera, J. L., Martin, J. J., Risco, F., Garcia-Ochoa, S., Gamo, F. J., Sanz, L., Leon, L., Ruiz, J. R., Gabarro, R., Mallo, A., and Gomez de las Heras, F. (2004) Identification and activity of a series of azole-based compounds with lactate dehydrogenase-directed anti-malarial activity, *J. Biol. Chem. 279*, 31429−31439.
8. Winter, V. J., Cameron, A., Tranter, R., Sessions, R. B., and Brady, R. L. (2003) Crystal structure of *Plasmodium berghei* lactate dehydrogenase indicates the unique structural differences of these enzymes are shared across the *Plasmodium* genus, *Mol. Biochem. Parasitol. 131*, 1−10.
9. Dunn, C. R., Banfield, M. J., Barker, J. J., Higham, C. W., Moreton, K. M., Turgut-Balik, D., Brady, R. L., and Holbrook, J. J. (1996) The structure of lactate dehydrogenase from *Plasmodium falciparum* reveals a new target for anti-malarial design, *Nat. Struct. Biol. 3*, 912−915.
10. Read, J. A., Winter, V. J., Eszes, C. M., Sessions, R. B., and Brady, R. L. (2001) Structural basis for altered activity of M- and H-isozyme forms of human lactate dehydrogenase, *Proteins 43*, 175−185.
11. Kavanagh, K. L., Elling, R. A., and Wilson, D. K. (2004) Structure of *Toxoplasma gondii* LDH1: active-site differences from human lactate dehydrogenases and the structural basis for efficient $APAD^+$ use, *Biochemistry 43*, 879−889.
12. Dunn, C. R., Wilks, H. M., Halsall, D. J., Atkinson, T., Clarke, A. R., Muirhead, H., and Holbrook, J. J. (1991) Design and synthesis of new enzymes based on the lactate dehydrogenase framework, *Philos. Trans. R. Soc. London, Ser. B 332*, 177−184.
13. Hewitt, C. O., Eszes, C. M., Sessions, R. B., Moreton, K. M., Dafforn, T. R., Takei, J., Dempsey, C. E., Clarke, A. R., and Holbrook, J. J. (1999) A general method for relieving substrate inhibition in lactate dehydrogenases, *Protein Eng. 12*, 491−496.
14. Brown, W. M., Yowell, C. A., Hoard, A., Vander Jagt, T. A., Hunsaker, L. A., Deck, L. M., Royer, R. E., Piper, R. C., Dame, J. B., Makler, M. T., and Vander Jagt, D. L. (2004) Comparative structural analysis and kinetic properties of lactate dehydrogenases from the four species of human malarial parasites, *Biochemistry 43*, 6219−6229.
15. Piper, R., Lebras, J., Wentworth, L., Hunt-Cooke, A., Houze, S., Chiodini, P., and Makler, M. (1999) Immunocapture diagnostic assays for malaria using *Plasmodium* lactate dehydrogenase (pLDH), *Am. J. Trop. Med. Hyg. 60*, 109−118.
16. Makler, M. T., and Hinrichs, D. J. (1993) Measurement of the lactate dehydrogenase activity of *Plasmodium falciparum* as an assessment of parasitemia, *Am. J. Trop. Med. Hyg. 48*, 205−210.
17. Turgut-Balik, D., Shoemark, D. K., Moreton, K. M., Sessions, R. B., and Holbrook, J. J.. (2001) Over-production of lactate dehydrogenase from *Plasmodium falciparum* opens a route to new antimalarials, *Biotechnol. Lett. 23*, 917−921.
18. Turgut-Balik, D., Akbulut, E., Shoemark, D. K., Celik, V., Moreton, K. M., Sessions, R. B., Holbrook, J. J., and Brady, R. L. (2004) Cloning, sequence and expression of the lactate dehydrogenase gene from the human malaria parasite, *Plasmodium vivax*, *Biotechnol. Lett. 26*, 1051−1055.
19. Otwinowski, Z., and Minor, W. (1997) Processing of X-ray diffraction data collected in oscillation mode, *Methods Enzymol. 276*, 307−326.
20. Navaza, J. (1994) AmoRe: an automated package for molecular replacement, *Acta Crystallogr. A50*, 157−163.
21. Collaborative Computational Project (1994) The CCP4 suite: programs for protein crystallography, *Acta Crystallogr. D50*, 760−763.
22. Emsley, P., and Cowtan, K. (2004) Coot: model-building tools for molecular graphics, *Acta Crystallogr.. Sect. D: Biol. Crystallogr. 60*, 2126−2132.
23. Laskowski, R. A., MacArthur, M. W., Moss, D. S., and Thornton, J. M. (1993) PROCHECK: a program to check the stereochemical quality of protein structures, *J. Appl. Crystallogr. 26*, 283−291.
24. Hooft, R. W., Vriend, G., Sander, C., and Abola, E. E. (1996) Errors in protein structures, *Nature 381*, 272.
25. Leatherbarrow, R. J. (1992) *Grafit v.3.0*.
26. Read, J. A., Wilkinson, K. W., Tranter, R., Sessions, R. B., and Brady, R. L. (1999) Chloroquine binds in the cofactor binding site of *Plasmodium falciparum* lactate dehydrogenase, *J. Biol. Chem. 274*, 10213−10218.
27. Conners, R., Schambach, F., Read, J., Cameron, A., Sessions, R. B., Vivas, L., Easton, A., Croft, S. L., and Brady, R. L. (2005) Mapping the binding site for gossypol-like inhibitors of *Plasmodium falciparum* lactate dehydrogenase, *Mol. Biochem. Parasitol. 142*, 137−148.
28. Gomez, M. S., Piper, R. C., Hunsaker, L. A., Royer, R. E., Deck, L. M., Makler, M. T., and Vander Jagt, D. L. (1997) Substrate and cofactor specificity and selective inhibition of lactate dehydrogenase from the malarial parasite *P. falciparum*, *Mol. Biochem. Parasitol. 90*, 235−246.
29. Eszes, C. M., Sessions, R. B., Clarke, A. R., Moreton, K. M., and Holbrook, J. J. (1996) Removal of substrate inhibition in a lactate dehydrogenase from human muscle by a single residue change, *FEBS Lett. 399*, 193−197.
30. Vander Jagt, D. L., Hunsaker, L. A., and Heidrich, J. E. (1981) Partial purification and characterization of lactate dehydrogenase from *Plasmodium falciparum*, *Mol. Biochem. Parasitol. 4*, 255−264.
31. Reddy, S. G., Scapin, G., and Blanchard, J. S. (1996) Interaction of pyridine nucleotide substrates with *Escherichia coli* dihydrodipicolinate reductase: thermodynamic and structural analysis of binary complexes, *Biochemistry 35*, 13294−13302.
32. Hewitt, C. O., Sessions, R. B., Dafforn, T. R., and Holbrook, J. J. (1997) Protein engineering tests of a homology model of *Plasmodium falciparum* lactate dehydrogenase, *Protein Eng. 10*, 39−44.
33. Dando, C., Schroeder, E. R., Hunsaker, L. A., Deck, L. M., Royer, R. E., Zhou, X., Parmley, S. F., and Vander Jagt, D. L. (2001) The kinetic properties and sensitivities to inhibitors of lactate dehydrogenases (LDH1 and LDH2) from *Toxoplasma gondii*: comparisons with pLDH from *Plasmodium falciparum*, *Mol. Biochem. Parasitol. 118*, 23−32.
34. DeLano, W. L. (2002) *The PyMOL Molecular Graphics System*, DeLano Scientific, San Carlos, CA.

BI051416Y